Deployable membranes designed from folding tree leaves

By D. S. A. De Focatiis† and S. D. Guest

*Department of Engineering, University of Cambridge,
Trumpington Street, Cambridge CB2 1PZ, UK*

Published online —

A simple model of deploying tree leaves is assembled in different arrangements to produce polygonal foldable membranes for use as deployable structures. One family of folding patterns exhibits a small strain mechanism, which is investigated. Variations on the basic arrangements can be used to fold membranes with a discretized curvature.

**Keywords: Miura-Ori; leaf opening; folding structure;
deployable structure; reflector dish; solar panel**

1. Introduction

The analysis of tree leaves as engineering structures is a relatively recent one. Most leaves can be modelled as thin membranes or laminae with reinforcements in the form of veins and midribs. It is necessary for the thin membrane to fold in the wind to decrease drag and subsequent mechanical damage (Vogel 1989). However, it is also necessary for leaves to sustain their own weight and other small loads (Niklas 1992). The leaf is therefore a compromise in flexibility and rigidity. It is the interaction of these stiffening members and the flexible membrane panels that leads to an interesting mechanism.

Tree leaves have been shown to exhibit a deployment mechanism to allow the young leaves to fit inside the small buds. Hornbeam and beech leaves have a particularly simple and regular corrugation pattern (Kobayashi *et al.* 1998). This pattern is strengthened by the distortion induced in the cantilevered corrugation (Kresling 2000). Maple leaves have a more complex pattern, involving seven elements of corrugation, each connected to its neighbour (Kobayashi *et al.* 2000).

Folding patterns for membranes have previously been considered in the field of aerospace structures. Two examples are a two-dimensional deployable array, known as the *Miura-Ori*, which has application as a solar panel (Miura & Natori 1985), and the wrapping of a membrane around a central hub, known as the *wrapping-fold pattern*, which has been considered for a solar sail structure (Guest & Pellegrino 1992).

This paper investigates the effect of combining several corrugated leaf patterns in order to produce deployable surfaces, such as solar panels, antennas, solar sails,

† Present address: Department of Engineering Science, Oxford University, Oxford OX1 3PJ, UK (davide.defocatiis@eng.ox.ac.uk).
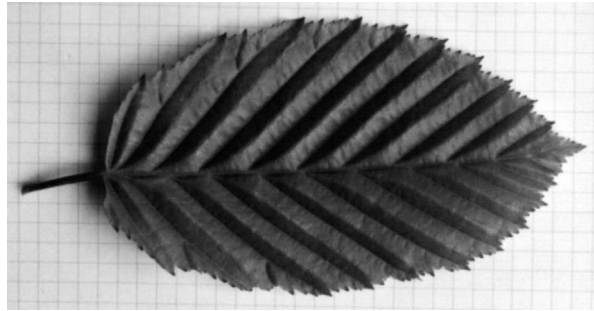
Figure 1. A typical hornbeam leaf, showing the corrugations. (Reproduced with permission from J. F. V. Vincent (Kobayashi *et al.* 1998).)

folding tents and roof structures. The advantage of the leaf-folding patterns is seen when several membranes exhibiting the folding pattern of the leaf are joined side by side to produce polygons. The leaves can be arranged in two basic ways, either pointing towards the centre of the polygon, *leaf-in*, or directed away from it, *leaf-out*. The folds of different leaves are interconnected and compatible with each other, and the whole structure can be folded and unfolded from a single or multiple driving points.

The *leaf-in* pattern has a small amount of distortion induced by the unfolding process, which is studied and quantified. This distortion is a small strain mechanism which can be used to the advantage of the structure, creating a bistability in the deploying membrane.

Simple approximations to curved surfaces may be folded for applications such as satellite reflector dishes.

2. The folding patterns

(*a*) *The one-leaf unit*

The simple model of deploying tree leaves consists of a corrugated surface of alternating crest and valley folds, meeting the midrib at an angle α. This type of folding pattern is especially evident in hornbeam leaves (figure 1).

This model has been used to gain an understanding of timing in leaf development (Kobayashi *et al.* 1998). The model is shown with crest folds being represented by solid lines and valley folds by dashed lines (figure 2).

This type of folding pattern is a simple form of the corrugated surface known as the *Miura-Ori* (Miura 1980), and is interesting because it allows simultaneous extension in two perpendicular directions. A model is shown in various stages of deployment (figure 3).

(*b*) *The leaf-out pattern*

One way of arranging the leaves to form a larger membrane is with the stems meeting at a point: this is henceforth referred to as the *leaf-out* pattern, as the leaves point outwards from the centre. The number of leaves in the pattern is denoted as n, and the number of membranes, or segments, between the veins on either side of the midrib is denoted as s (figure 4).
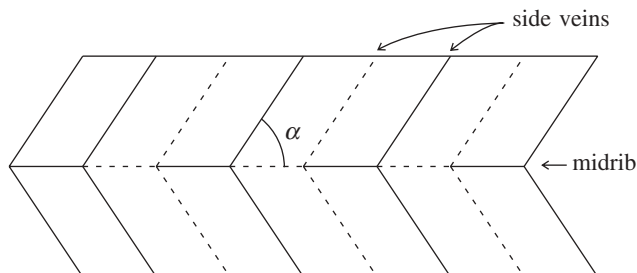
Figure 2. The fold lines in a corrugated leaf model. Solid lines indicate crest folds and dashed lines indicate valley folds. The angle between the midrib and the side veins, known as the vein angle, is α.
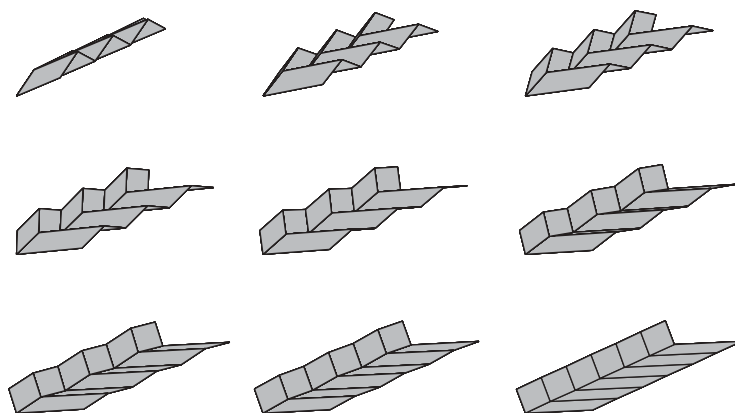

Figure 3. Nine stages in the deployment of the leaf-folding pattern.
The structure extends simultaneously in two directions.

For a planar membrane, the relationship for the *leaf-out* pattern between n and α is

$$n = \pi/\alpha. \tag{2.1}$$

A paper model has been assembled by scoring the paper to aid the folding. A typical deployment shows the obvious elongation in two mutually perpendicular directions (figure 5).

In order to minimize the size of the folded structure, there must be maximum overlap in the folding panels. The optimal folding shape is observed to be that of an n-sided polygon. Hence, for the example shown in figures 4 and 5, the membrane is square.

(c) The leaf-in pattern

Another way of arranging leaves to form a membrane is with the tips meeting at a point: this is henceforth referred to as the *leaf-in* pattern, as the leaves point towards the centre. An example is shown in figure 6. The number of leaves and segments are defined as before, by n and s, respectively.
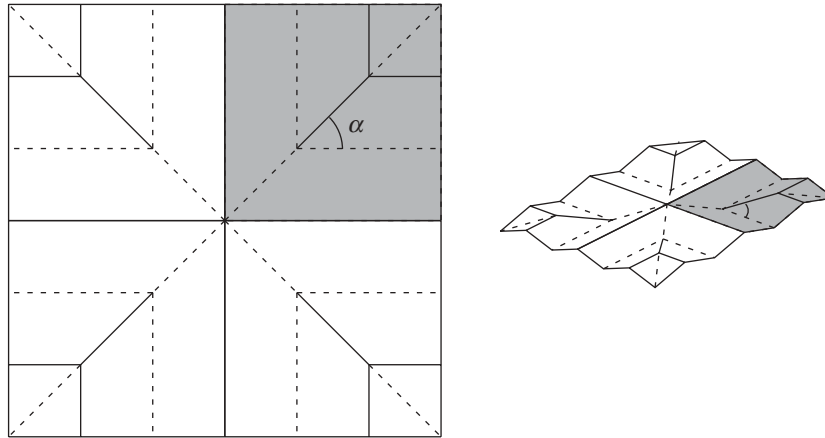
Figure 4. Leaves pointing away from the centre, the *leaf-out* pattern. One 'leaf' is shown shaded. There are four leaves and three segments either side of the midrib per leaf; $n = 4$, $s = 3$, $\alpha = 45°$.
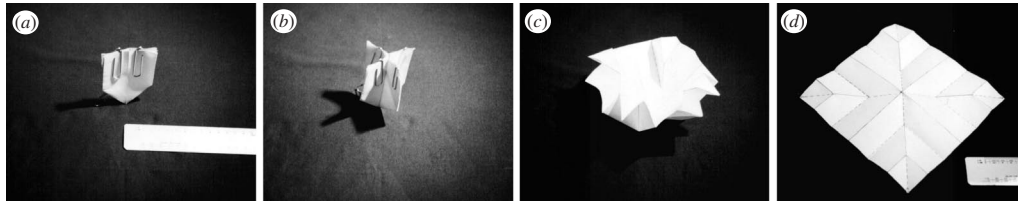

Figure 5. The deployment of a *leaf-out* pattern paper model, in four stages ((*a*)–(*d*)); $n = 4$, $s = 3$, $\alpha = 45°$.
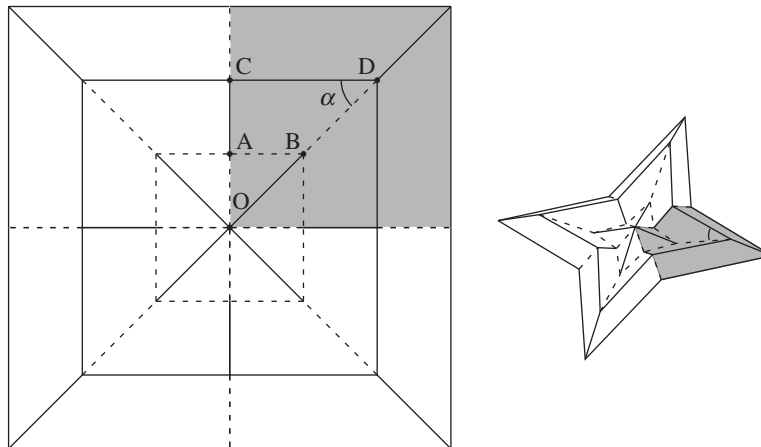

Figure 6. Leaves pointing towards the centre: the *leaf-in* pattern. One 'leaf' is shown shaded. This arrangement has $n = 4$, $s = 3$, $\alpha = 45°$.

The basic structure assumes that the side folds are continuous fold lines between adjoining leaves. This requires the following relationship between α and n:
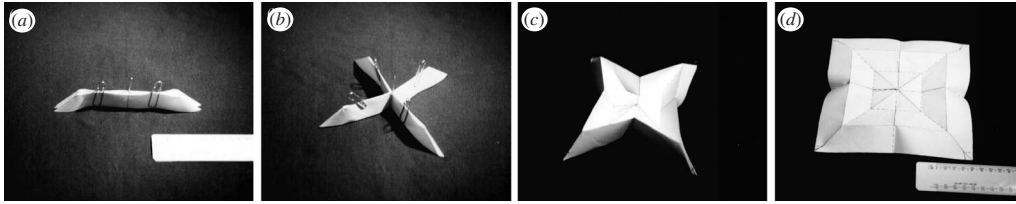
$$\alpha = \frac{\pi}{2} - \frac{\pi}{n}. \tag{2.2}$$

Figure 7. The deployment of a *leaf-in* pattern paper model,
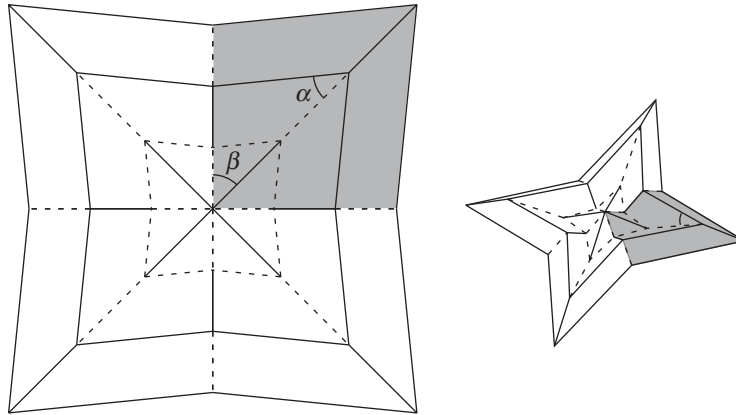in four stages ((a)–(d)); $n = 4$, $s = 3$, $\alpha = 45°$.

Figure 8. A *skew leaf-in* pattern with $\alpha = r(\pi/2 - \pi/n)$, where $r \leqslant 1$.
One leaf is shown shaded. $n = 4$, $s = 3$, $r = \frac{8}{9}$, $\alpha = 40°$.

This produces directly the shape of the deployed membrane as that of an n-sided polygon, as in the *leaf-out* pattern.

A paper model has been assembled in the same way as the previous model. The deployment also occurs in two mutually perpendicular directions (figure 7). It is observed that there is some strain in the paper during the unfolding process.

(d) The skew leaf-in pattern

A variation on the *leaf-in* pattern consists of changing the angle of the fold lines while retaining the same number of leaves. The angle α can be allowed to vary from the initial value of $(\pi/2) - (\pi/n)$. Paper models show that it is not possible to increase the angle α if the paper is to fold. It is possible, however, to reduce the value of α to

$$\alpha = r\left(\frac{\pi}{2} - \frac{\pi}{n}\right), \quad 0 \leqslant r \leqslant 1. \tag{2.3}$$

This pattern is known as the *skew leaf-in* pattern, and results in the side folds no longer being continuous (figure 8).

The paper model has shown that the deployment of the *skew leaf-in* pattern is smoother than the *leaf-in* pattern for equivalent parameters (figure 9). The main difference between the *skew leaf-in* pattern and the *leaf-in* pattern is that this structure is unable to fold fully closed (figures 7a and 9a).
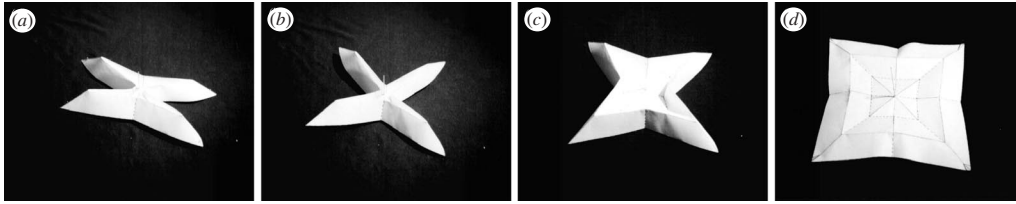
Figure 9. The deployment of a *leaf-in* pattern paper model with $r \leqslant 1$ in four stages $((a)–(d))$; $n = 4$, $s = 3$, $r = \frac{8}{9}$, $\alpha = 40°$.
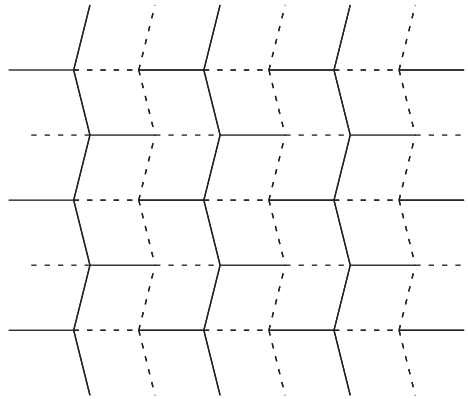

Figure 10. The infinite folding surface produced from the *skew leaf-in* pattern for $n \to \infty$, known as *Miura's folded map*.

(*e*) *Miura's folded map*

The special case of the *skew leaf-in* pattern when $n \to \infty$ produces an infinite surface where leaves are put side by side along a straight line (figure 10). The folding arrangement corresponds to the pattern known as *Miura's folded map* (Miura 1980).

3. Further analysis of the *leaf-in* pattern

(*a*) *The folding incompatibility*

Close inspection of the folding arrangement of any *leaf-in* pattern will reveal an incompatibility during the folding. While the pattern can exist strain-free in both the folded and unfolded configurations, the folding stages require a small amount of distortion. The distortion is observed to be a combination of bending and shear in the panels and rolling movement of the fold lines in order to accommodate the folding. In the paper models the distortion is seen by the buckling of the panels and the wear in the fold lines.

To illustrate the reasons for this incompatibility, the points marked as A and B on figure 6 are shown folding in figure 11a,b. The fold angle, γ, is the smaller angle between the fold lines: $\gamma = 90°$ for point A, and $\gamma < 90°$ for point B. Any pattern is made up of a number of different folds. For example, in the specific pattern shown in figure 6, point A folds have $\gamma = 90°$ and point B folds have $\gamma = \alpha = 45°$.

While the folds about point B (figure 11b) have a smooth, continuous folding operation, the folds about point A (figure 11a) fold in two distinct stages. When
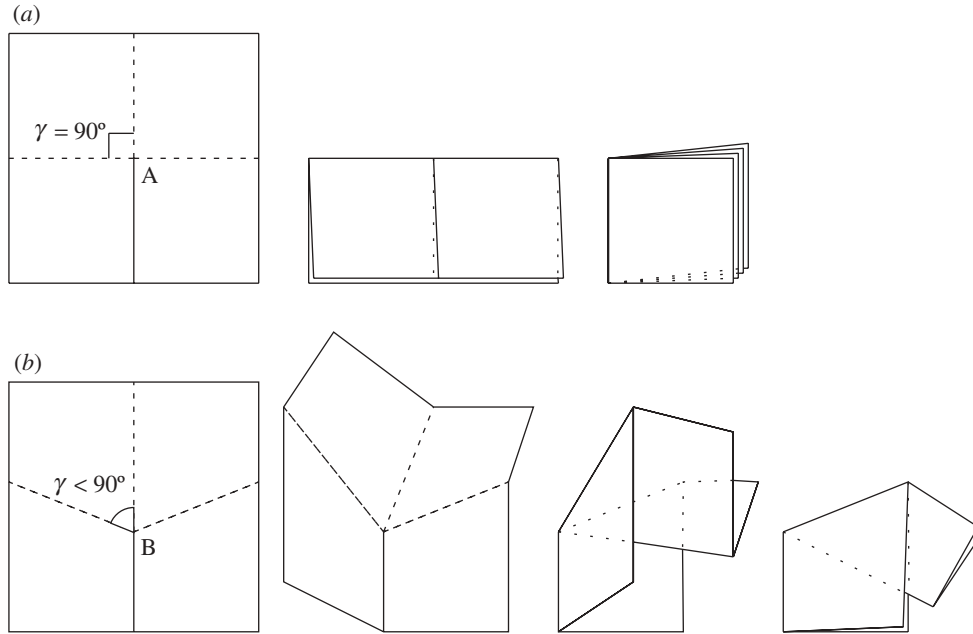
(*a*)

(*b*)

Figure 11. Two types of fold-line junctions. (*a*) $\gamma = 90°$, a two step folding process.
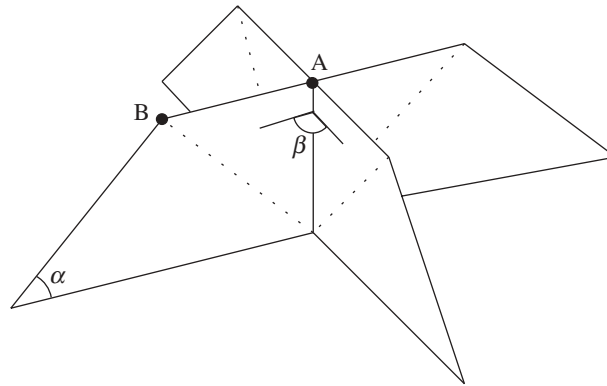(*b*) $\gamma < 90°$, a smooth, continuous folding operation.

Figure 12. The initial angle between folded leaves at A is $\beta = 2\pi/n$.
The fold at B has yet to begin unfolding.

two fold lines meet at right angles, folding is not a single step, but the sequential two steps of the simplest, one-line folding. Hence it is clear that the folds around A and B cannot unfold simultaneously (Miura 1991); if these structures were to be constructed out of rigid members, they would not be able to fold at all. In reality, however, it has been shown by the paper models of the patterns that the folding *is* able to take place, but this must involve some small deformation of the fold pattern.

Observation from paper models indicates that the strains are increased as the number of leaves n is increased. When the structure is fully folded, there is an initial angle β at the central vertex between successive leaves, shown in figure 12, and given
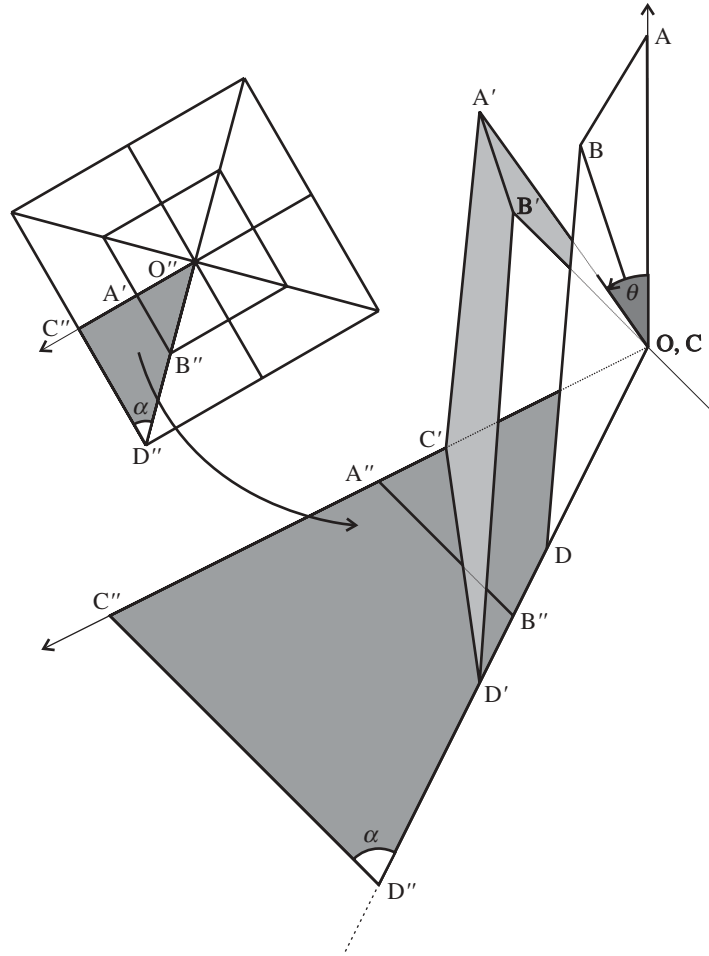
Figure 13. The deployment of two segments, fully closed (ABCD), deploying (A′B′C′D′) and fully deployed (A″B″C″D″). OA, OB, AB, AC and BD are assumed rigid, except CD, whose length is evaluated as a function of the opening angle, θ.

by

$$\beta = 2\pi/n. \tag{3.1}$$

This corresponds to the angle through which the first stage of unfolding at A has gone before the beginning of the deployment. Before the folds at B can begin unfolding, the first stage of unfolding at A must be completed. For large values of n, angle β is small, thus inhibiting the unfolding of point B. For small values of n, angle β is bigger, and thus the point A fold has almost completed its first stage of unfolding, and is able to proceed to the second stage and unfold fully together with point B with less strain.

Observation of paper models of *leaf-in* patterns and *skew leaf-in* patterns has shown that 'skew' patterns fold with smaller strains than the equivalent $r = 1$ patterns.
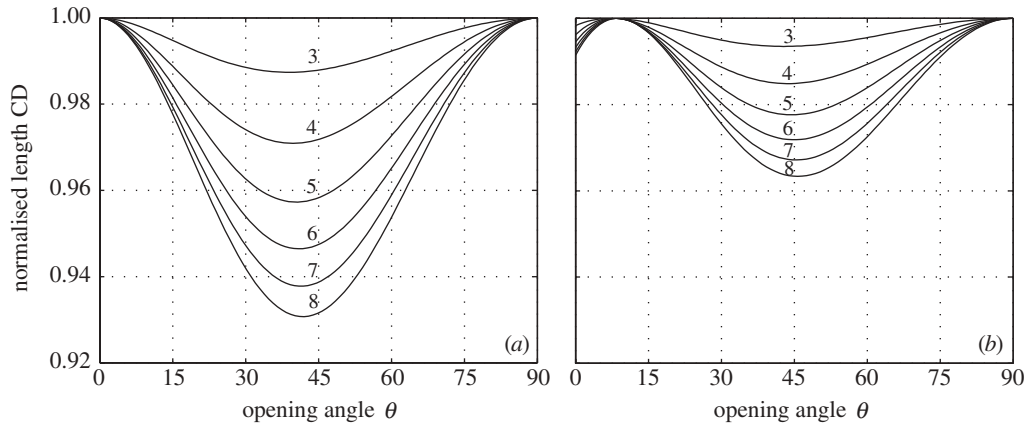
Figure 14. Relationship between the normalized length, CD, and the opening angle, θ, for (*a*) $r = 1$ *leaf-in* and (*b*) $r = \frac{8}{9}$ *skew leaf-in*.

(*b*) *A simple analysis of the folding incompatibility*

In practice, the deployment of the paper models indicates complex strain interactions between the panels and the folds. For the purpose of analysis, a simple model considering only two segments, $s = 2$, is used to observe the relative incompatibility for different fold patterns. The deployment is assumed to be fully symmetric, and hence only one half of one leaf is modelled. Two segments are considered because this is the minimum required for the incompatibility to appear. The unfolding of a one-segment membrane exhibits no strains.

The fold pattern is modelled as a series of bars OA, OB, AB, AC, BD and CD connected by spherical joints. To simplify the modelling as much as possible, all of the bars are assumed to be rigid, except CD: the change of length in bar CD is therefore a measure of the incompatibility. A further simplification is to assume that points C and D remain on the same horizontal plane as the origin O during the deployment. Figure 13 shows the deployment of the two segments from ABCD (fully folded) to A′B′C′D′ (partly deployed) to A″B″C″D″ (fully deployed). The measure of deployment is the opening angle θ, defined as the angle between OA and the vertical.

With the assumptions made, the system of bars becomes a one-degree-of-freedom mechanism, and it is a matter of geometry to find the length CD as a function of θ.

In order to compare different n values, the length CD is normalized to unity when fully deployed. The shortening is evaluated for the range of values of the opening angle θ. Figure 14 shows the relationship between the opening angle θ and the normalized spring length S for different n for two different fold patterns.

Figure 14*a* verifies that the $r = 1$ structure is compatible, or stress free, at the extremes $\theta = 0°$ and $\theta = 90°$. Figure 14*b* shows that, for $r = \frac{8}{9}$, the structure is compatible for $\theta = 90°$, but at $\theta = 0°$ there is deformation. As is observed from the paper models, the structure is unable to fold fully closed but there is a second compatible point at $\theta \approx 9°$.

The figures also show that the peak strain in folding is reduced to *ca.* 50% of its original value by varying r from 1 to $\frac{8}{9}$, confirming the observations from the paper models.
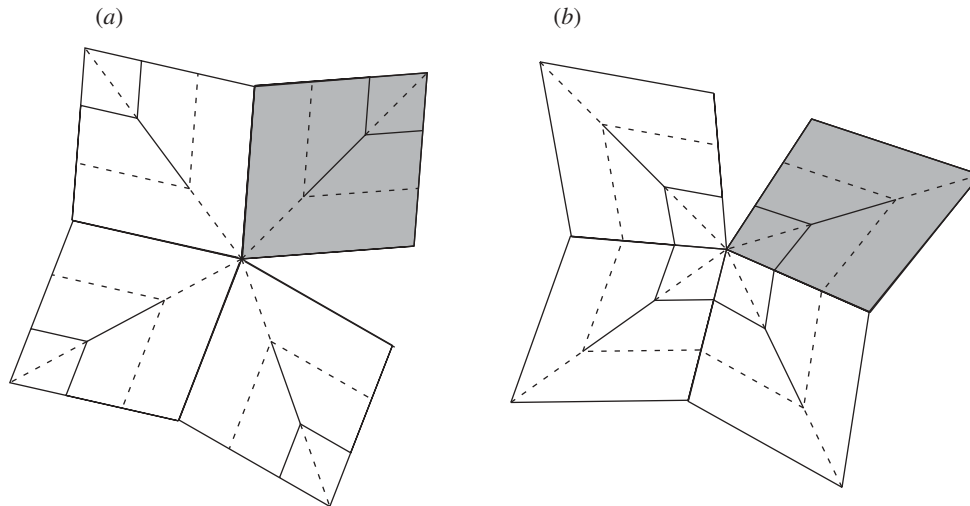
(*a*)   (*b*)

Figure 15. Two examples of patterns with an angular defect at the centre simulating curvature. One 'leaf' is shown shaded. (*a*) *Leaf-out* pattern, $n = 4$, $s = 3$, $\alpha = 40°$. (*b*) *Leaf-in* pattern, $n = 4$, $s = 3$, $r = \frac{8}{9}$, $\alpha = 40°$.

(*c*) *Further observations*

Paper models indicate that, for structures with $s > 2$, the deployment tends to occur in stages. The inner segments open before the outer segments. It is noted from observation of a larger paper model, $n = 8$, $s = 6$, that the deploying structure exhibits some stability as each segment is unfolded, beginning with the central segments. The structure is stress free and at a minimum strain energy level when it is fully folded and when it is fully unfolded, but there appear to be a number of local energy minima along the deployment path. Simple models, along the lines of that described in § 3 *b*, are not able to capture these details; to do so it is necessary to consider the system as a set of connected panels.

4. Folding a curved surface

Many applications, such as reflector dishes, require the use of curved surfaces. Folding and packaging truly curved panels is a difficult problem (see, for example, Guest & Pellegrino 1996) that completely invalidates the approach followed here. An alternative approach is to approximate the surface as a number of flat panels, and introduce a suitable angular defect at vertices; this approach can be followed for the fold patterns considered in this paper.

Two very simple paper models have been made, where a curvature approximation is introduced as a single angular defect at the centre of the model. Figure 15 shows the fold patterns that were used; the free edges were joined during assembly. The deployment of the models is shown in figure 16. Two features are worth noting.

(1) The *leaf-out* structure is still able to fold fully closed.

(2) While the deployment of the *leaf-out* structure still occurs in a single smooth movement, that of the *leaf-in* structure requires an additional deployment hur-
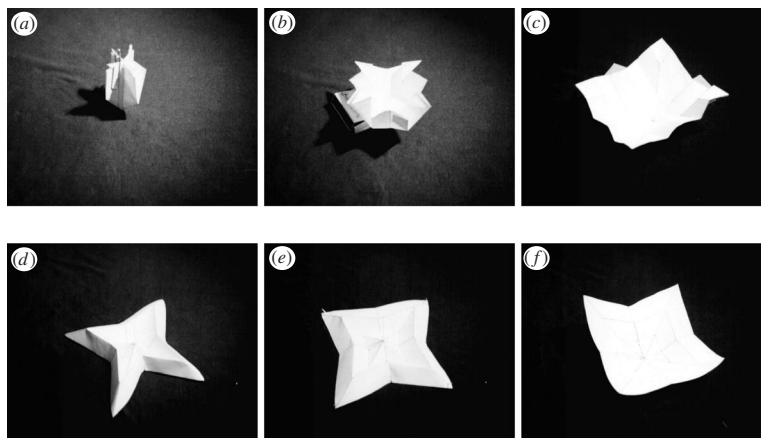
Figure 16. The deployment of structures with an angular defect to simulate curvature. A *leaf-out* structure ((*a*)–(*c*)) and a *leaf-in* structure ((*d*)–(*f*)). Note the additional *snap-through* stage required by the leaf-in structure between (*e*) and (*f*); $n = 4$, $s = 3$.

dle: it needs to *snap through* the final corrugated stage to achieve the desired curvature (figure 16*e*, *f*).

5. Conclusions

This paper has presented a very preliminary study of two new fold patterns for thin membrane structures that are genuinely biomimetic. They were developed by considering how the folding of a natural structure (a leaf) could be extended to engineering structures. Clearly much further study is required before these fold patterns could be used for actual deployable structures, but they do provide a new approach to a common packaging problem.

References

Guest, S. D. & Pellegrino, S. 1992 Inextensional wrapping of flat membranes. In *Proc. 1st Int. Sem. on Structure and Morphology, Montpellier, France, 7–11 September 1992* (ed. R. Motro & T. Wester), pp. 203–215. LMGC, Université Montpellier II.

Guest, S. D. & Pellegrino, S. 1996 A new concept for solid surface deployable antennas. *Acta Astronaut.* **38**, 103–113.

Kobayashi, H., Kresling, B. & Vincent, J. F. V. 1998 The geometry of unfolding tree leaves. *Proc. R. Soc. Lond.* B **265**, 147–154.

Kobayashi, H., Daimaruya, M. & Vincent, J. F. V. 2000 Folding/unfolding manner of tree leaves as a deployable structure. In *Proc. IUTAM–IASS Symp. on Deployable Structures, Theory and Applications* (ed. S. Pellegrino & S. D. Guest). Kluwer.

Kresling, B. 2000 Coupled mechanisms in biological deployable structures. In *Proc. IUTAM–IASS Symp. on Deployable Structures, Theory and Applications* (ed. S. Pellegrino & S. D. Guest), pp. 229–238. Kluwer.

Miura, K. 1980 Method of packaging and deployment of large membranes in space. In *Proc. 31st Congr. Int. Astronautics Federation, Tokyo, Japan*, pp. 1–10.

Miura, K. 1991 A note on the intrinsic geometry of origami. In *Proc. 1st Int. Conf. of Origami Science and Technology, Ferrara, Italy, 6–7 December 1989, pp. 239–249.* Humiaki Huzita.

Miura, K. & Natori, M. 1985 2-D array experiment on board a space flyer unit. *Space Solar Power Rev.* **5**, 345–356.

Niklas, K. J. 1992 *Plant biomechanics: an engineering approach to plant form and function.* Chicago, IL: University of Chicago Press.

Vogel, S. 1989 Drag and reconfiguration of broad leaves in high winds. *J. Exp. Bot.* **40**, 941–948.